High-Resolution GNSS-Tracked Drifter for Studying Surface Dispersion in Shallow Water

KABIR SUARA, CHARLES WANG, YANMING FENG, AND RICHARD J. BROWN

Science and Engineering Faculty, Queensland University of Technology, Brisbane, Queensland, Australia

HUBERT CHANSON

School of Civil Engineering, University of Queensland, Brisbane, Queensland, Australia

MICHAEL BORGAS

Marine and Atmospheric Research, Commonwealth Scientific and Industrial Research Organisation, Aspendale, Victoria, Australia

(Manuscript received 30 June 2014, in final form 6 November 2014)

ABSTRACT

The use of Global Navigation Satellite System (GNSS)-tracked Lagrangian drifters allows more realistic quantification of fluid motion and dispersion coefficients than Eulerian techniques because such drifters are analogs of particles that are relevant to flow field characterization and pollutant dispersion. Using the fast-growing real-time kinematic (RTK) positioning technique derived from GNSS, drifters are developed for high-frequency (10 Hz) sampling with position estimates with centimeter accuracy. The drifters are designed with small size and less direct wind drag to follow the subsurface flow that characterizes dispersion in shallow waters. An analysis of position error from stationary observation indicates that the drifter can efficiently resolve motion up to 1 Hz. The result of the field deployments of the drifter in conjunction with acoustic Eulerian devices shows a higher estimate of the drifter streamwise velocities. Single particle statistical analysis of field deployments in a shallow estuarine zone yielded estimates of dispersion coefficients comparable to those of dye tracer studies. The drifters capture the tidal elevation during field studies in a tidal estuary.

1. Introduction

The Lagrangian technique is known to provide conceptual data for observing the spatial structure of the flow field in water bodies. These data are obtainable either by visualization of spreading dye or the position history of water-following parcels known as drifters. The Lagrangian technique allows a more realistic estimate of the scale of motion and diffusion coefficient than the Eulerian technique because it focuses on the motion of particles of interest. These estimates are particularly important in marine ecological studies (Landry et al. 2009; Qiu et al. 2010) and safety measures, for example, in the investigation of fate of contaminants (Kopasakis et al. 2012).

Corresponding author address: Kabir Suara, Science and Engineering Faculty, Queensland University of Technology, 2 George St., Brisbane QLD 4000, Australia.
E-mail: k.suara@qut.edu.au

DOI: 10.1175/JTECH-D-14-00127.1

In riverine and estuarine environments, a number of theoretical and empirical dispersion models from downstream observation of injection concentration using tracer probes are available in the literature (Fischer et al. 1979; Chanson 2004; Sundermeyer and Ledwell 2001; Situ and Brown 2013). Tracers rapidly mix in a vertical direction as compared to transverse direction due to the large width-to-depth ratio of shallow waters (Swick and MacMahan 2009); thus, vertical mixing is often inferred. With tracer technology, accurate estimation of the transverse mixing simplifies the advection–diffusion equation to a one-dimensional form in order to predict the longitudinal dispersion. However, these environments are usually unsteady with complex bathymetry and a high level of human activities, and thus require regular monitoring.

Lagrangian drifters–floats have been widely applied to fluid dynamics for oceans (Ohlmann et al. 2012; Berti et al. 2011; Poje et al. 2014), lakes (Pal et al. 1998; Stocker and Imberger 2003), and nearshore and coastal regions (List et al. 1990; Spydell and Feddersen 2009; Landry et al. 2009; Schroeder et al. 2012). Evaluation of Surface Velocity Program (SVP) drifters applied to ocean and large water bodies is available in Lumpkin and Pazos (2007). The scale of motion that can be resolved greatly depends on the size of the parcel and precision of position estimates. Removal of selective availability—an intentional addition of white noise to the global positioning system (GPS) satellite signal—by the U.S. government on 2 May 2000 reduced the position error estimation from 100 to 20 m (D'Roza and Bilchev 2003; Johnson et al. 2003) and has made it possible for GPS drifters to be used to studying surfzone dispersion with flow features on the order of 10 m (Johnson et al. 2003; Schmidt et al. 2003; Johnson and Pattiaratchi 2004). A drifter made from a handheld GPS unit described by MacMahan et al. (2009) could be used to resolve flow features in the order of 3 m. Integral length in a shallow water body (i.e., ones with depth limited to 2–3 m at high tide) is estimated by Chanson et al. (2014) to be in the order of 1 m, which requires drifters with centimeter range position accuracy sampled at high frequency.

Improvements in the position fixing of GPS-Global Navigation Satellite System (GNSS) has made accuracy at the level of centimeters possible with the use of the precise real-time kinematic (RTK) positioning algorithm and a nearby reference station for modeling and eliminating GPS measurement errors. An RTK data processing system, such as the open source software Real-Time Kinematic Library, RTKLib (Takasu and Yasuda 2009), allows for real-time download and processing of GPS-GNSS raw data using low-cost off-the-shelf hardware to derive precise positioning solutions (Takasu and Yasuda 2009). The RTK–GNSS system provides a promising technique for developing a high-resolution Lagrangian device that allows for effective resolution of flow features on the order of a few centimeters, and thus it could be used for studying dispersion in shallow waters and estuarine systems.

The aim of this paper is to describe the performance of evolving GNSS-tracked drifters with centimeter resolution, for studying dispersion in shallow water estuaries. The paper describes field observation in a typical estuarine system using these newly developed drifters deployed alongside a fixed acoustic Doppler velocimeter (ADV) and an acoustic Doppler current profiler (ADCP). The present configuration of the drifters is designed to follow the subsurface current that characterizes horizontal dispersion in shallow water. Also described in this paper are the results of single particle analysis of several field deployments of these drifters. The paper also describes the additional application in flood height monitoring while outlining possible limitations of the system.

2. Shallow water drifter design

Some primary design criteria for a shallow water drifter include small size, large drag area ratio, and stability during drift. Small size ensures that the drifter is capable of operating in water depth less than 1 m, minimizing the surface direct windage and easing the deployment and retrieval during field applications. Slip is the horizontal motion of a drifter that differs from the motion of currents (Lumpkin and Pazos 2007). The wind-induced current U_{slip} depends on both drifter drag area ratio and wind vector in the vicinity of the measurements. The U_{slip} can be described as

$$|U_{\mathrm{slip}}| = \frac{A}{R} U_{\mathrm{wind}}, \tag{1}$$

where R is the ratio of drag area (product of drag coefficient and cross-sectional area) of the submerged portion to that of the unsubmerged portion of the drifter, U_{wind} is the downwind speed ($\mathrm{m\,s^{-1}}$), and A = 0.07 (Niiler and Paduan 1995). Therefore, the slip could be minimized with large R, that is, minimized unsubmerged area with optimized submerged area.

The present drifter configuration is made of aluminum machined into a hollow cylinder with an outside diameter of 197 mm and a height of 260 mm (Fig. 1). Arranged close to the base of the cylindrical aluminum capsule are the GNSS receiver, the computing board, and direct current (dc) batteries to power the circuit boards arranged to provide ballasting. The drifter is additionally ballasted with steel plates to prevent overturning with positive buoyancy, such that only 30 mm from the tip of the hull is maintained above the water surface. This ensures vertical separation of centers of mass and buoyancy to reduce the heave and roll of the drifter. This configuration results in an estimated wind slip U_{slip} of 0.03–0.032 $\mathrm{m\,s^{-1}}$, assuming a wind of 5 $\mathrm{m\,s^{-1}}$ in the same direction as the drifter using the simple model in Eq. (1). Each drifter records and stores GNSS raw measurements (pseudorange and carrier phase data) at 10 Hz in the receiver for postprocessing. At this frequency, the batteries power the drifter for up to 12 h of deployment.

The spatial requirement of shallow water estuaries includes capturing the dispersion process on the order of the integral length scale, which is approximately half the depth of the channel. The small spatial [O(1 m)] and short temporal [O(30 s)] scales of interest in estuaries require centimeter accuracy with high-frequency [O(1 Hz)] data acquisition. At present, the drifter is made to store data in a Secure Digital card while a reference station acquires data simultaneously. Upon retrieval, the data are postprocessed in differential mode using RTKlib, which provides coordinates in geodetic

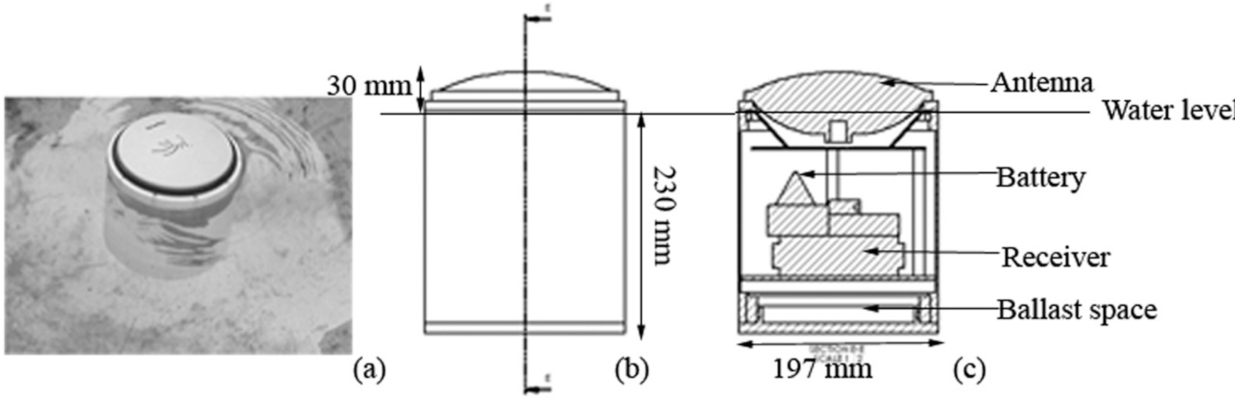

FIG. 1. (a) Photograph and (b) elevation of the GPS-tracked drifter, and (c) schematic section showing the arrangement of the internal components and the water level.

form. Further quality control is then implemented as described in section 4.

3. Field deployment

Two field studies were conducted in Eprapah Creek, a subtropical creek located to the southeast Queensland, Australia (Chanson et al. 2012). The estuarine zone is about 3.8 km long with a typical semidiurnal tidal pattern and flows into Moreton Bay, adjacent to the Pacific Ocean at Victoria Point (Trevethan et al. 2008). Based on a survey carried out on 30 September 2013, the creek has a maximum depth of 3–4 m mid-estuary at high tide with a width of about 50 m at site 1A close to Moreton Bay and 10 m at site 2C (Fig. 2).

On 30 August 2013, two drifters sampling at 10 Hz were deployed two times in a cluster in an incoming tide at the site enclosed in polyline (site 2; Fig. 2) and were

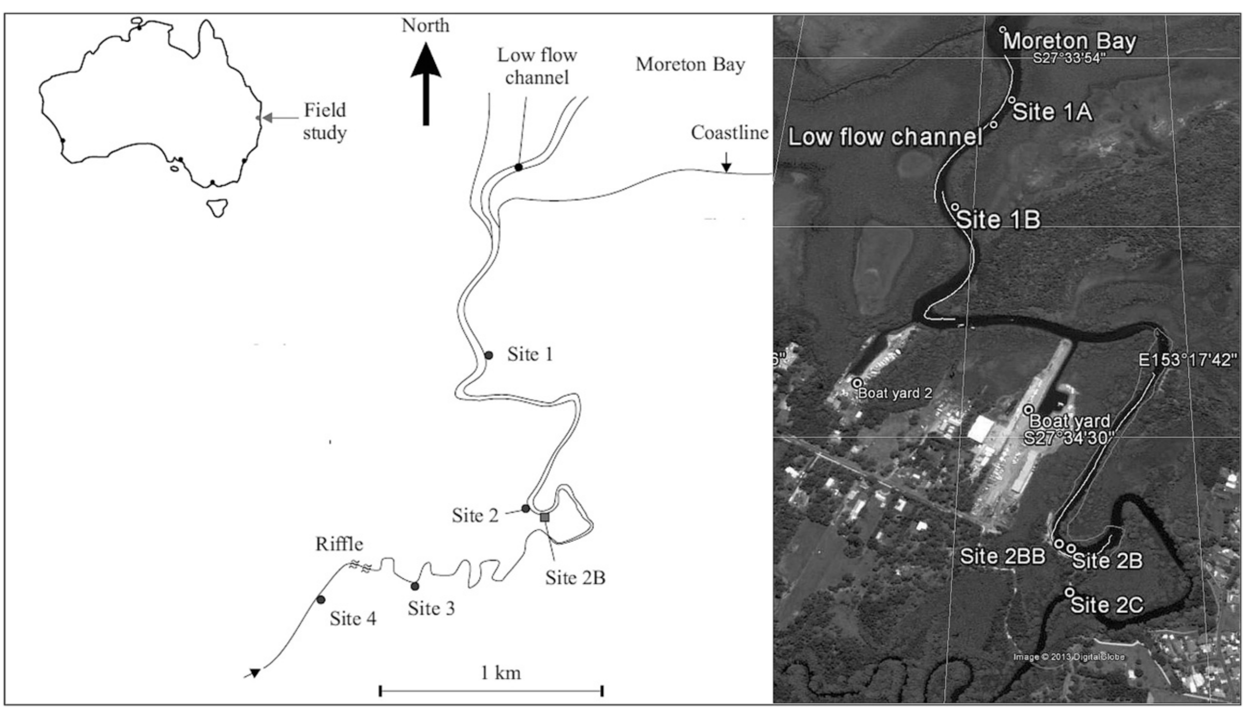

FIG. 2. (right) Google Earth vicinity map of Eprapah Creek with (left) schematic of features shown on right, as well as the general location within Australia of the study. At the top middle is the mouth of the creek close to Moreton Bay. Flood tide flows in from Moreton Bay through site 1A; the gray-shaded square, site 2BB, has a fairly straight portion and a semicircular meander where most deployments were carried out. White lines in right panel show trajectories of drifters. Eprapah Creek is located at −27.567°S, 153.30°E. Google Earth 7.1.2.2041.

TABLE 1. Summary of field deployments of drifter; wind data were taken using Vintage PRO weather station fixed at site 2.

Test	Date (2013)	Location	Drifter tracks	Total drift time (min)	Mean flow speed ($m\,s^{-1}$)	Mean wind speed ($m\,s^{-1}$)	Dominant wind direction	U_{slip} ($m\,s^{-1}$)
1	29 Aug	Site 2	4	200	0.143	1.93	NNE	±0.0121
2	30 Sep	Site 2B and 2BB	4	80	0.140	1.18	NNE	±0.0071
3	30 Sep	Site 1A	1	36	0.240	1.42	N	±0.0092
4	30 Sep	Site 1B	1	40	0.190	1.34	NNE	±0.0084
5	30 Sep	Site 2	1	50	0.150	1.01	NNE	±0.0060

allowed to float past the semicircular meander (site 2B) before retrieval. Also deployed was a fixed SonTek ADV at the end of the straight part of the channel 10 m from the left bank (Fig. 2). On 30 September 2013, several deployments were made in an outgoing tide from the upstream of site 2B (Fig. 2) past fixed devices for validation. Three SonTek 16-MHz micro-ADVs were similarly deployed at site 2B (Fig. 2). Note that this location was the most convenient for the setup because it has access to a boat launch and a solid bank for the data acquisition station. The three ADVs were placed at 0.32, 0.42, and 0.55 m from the bottom, respectively, and were about 11 m from the left bank of the channel. In addition, a Teledyne RD Instruments (RDI) Workhorse ADCP was deployed. The RDI Workhorse 1200-kHz self-logging ADCP was installed on the sediment–water interface in an upward-looking configuration. The ADCP was located at a transect 0.94 m lower than the bed elevation, 10.1 m downstream of the ADVs, and approximately 12.6 m from the left bank, and used a 0.05-m vertical bin size resulting into 55 bins. The ADCP ping rate was 5.56 Hz and produced averaged data over an 854-s interval. Additional drifter deployments were carried out at sites 1A and 1B (Fig. 2) to obtain an estimate of spatial mean velocity variation along the creek and the capability of the drifter in measuring tidal elevation. All drifter deployments were conducted from a small boat near the center of the channel using a wooden frame attached to the boat to reduce the bobbing effect and to provide estimates of initial distances between the drifters. Concurrently for both field trips, local tidal elevations were taken from a fixed location close to the ADV using survey staff. Table 1 summarizes the field conditions, the number of drifters, the number of successful deployments, the total drift times for the deployments, the mean velocities for each reach, and wind slips.

4. Data processing and coordinate transformation

The GNSS receivers of the drifters were configured to output 10-Hz raw measurements to be stored on the computing board for postprocessing using RTKlib, licensed under version 3 of the GNU General Public License (GPLv3; Takasu and Yasuda 2009). The RTK solution combined with the nearby reference station data achieves accuracy in the order of 1 cm for fixed solutions and about 10 cm for float solutions.

Like atmospheric flows, estuarine flows are anisotropic and the correct choice of coordinates is important (LaCasce 2008). Geographical coordinate frames are used for drifter studies in oceans and other large bodies, but they are not ideal for a statistical description of the channel due to sinuosity (Swick and MacMahan 2009), limited width, and strong streamwise velocity. From an east, north, up (e-n-u) coordinate, the time series were transformed to a channel-based streamwise, normal, up (s-n-u) coordinate using the MATLAB code provided by Legleiter and Kyriakidis (2006), with error limited to a few centimeters. Herein for simplification, the tidal direction is taken as positive streamwise, denoted by subscript "s"; the cross-shore n axis is normal to the channel centerline and positive toward the left bank, denoted by subscript "n"; and the u axis is taken as positive upward, denoted by subscript "u."

Quality control on the raw data includes removal of paths associated with disturbances; proximity to obstacles–banks of the channel; and cluster influence, based on the event record of field studies. It was observed from the field that spikes related to poor GPS fixes and external disturbances resulted in acceleration greater than $1.5\,m\,s^{-2}$ in the horizontal direction and $5\,m\,s^{-2}$ in the vertical direction. The time series of horizontal position coordinates (s, n) were processed by removing erroneous data with acceleration greater $1.5\,m\,s^{-2}$. These errors occurred when the number of satellites visible to the antenna permits the float solution (10-cm accuracy) instead of the fixed solution (1-cm accuracy). The vertical data are presented in meter Australian height datum (mAHD) and data with acceleration greater than $5\,m\,s^{-2}$ were flagged. Corrupted data in a time series could be replaced by spline fits and many other methods. Only about 2% of the data were flagged. These values were replaced by adding displacements corresponding to the mean track velocity to preceding positions. The velocities and accelerations used for the quality control were computed in a finite forward-differencing scheme with $N-1$ and $N-2$ degrees of freedom, respectively.

5. Evaluation of GPS system error

Errors in position fixing using GPS are associated with hardware, satellite clock error, and the multipath effect, among others. These errors have been minimized in the present drifter with the use of RTKlib software in real-time kinematic positioning mode, which corrects the location estimate of moving drifter with the error estimated by the reference station. However, this configuration still leaves some residual relative error associated with the acquisition unit, which has to be quantified for proper calibration of the device. To estimate the magnitude of the inherent error of the drifters, it was assumed that GPS position fixing is independent of drifter motion. The actual measurement x of a continuous observation X is obtained by deducting the relative error r [Eq. (2)]. Therefore, stationary observation is representative of the error in motion when $x = 0$. Three stationary tests at different open locations, each ranging from 25 to 45 min in length, were carried out with a drifter coupled with all internal components and sampling at a frequency of 10 Hz,

$$x = X - r \tag{2}$$

Position coordinates were transformed to a local enu coordinate and demeaned to obtain the relative errors shown (Fig. 3a). The maximum northing and easting position deviations were 0.025 and 0.018 m with maximum standard deviations of 0.01 and 0.008 m, respectively. The velocities of the relative errors were computed by central differencing (Fig. 3b) with magnitudes of $3.4 \times 10^{-5} \pm 0.0073$ and $2.14 \times 10^{-5} \pm 0.0056\,\mathrm{m\,s^{-1}}$, respectively, for test 1. Table 2 shows the error estimates from other locations. The stationary estimates were taken from locations within a 20-km radius of the designated reference station. Thus, the stationary position estimate is representative of the relative error and can therefore be used for quality control of the drifter deployments made within a 20-km differential range.

The low mean values indicate the symmetrical nature of relative position errors about the mean. 1The standard deviations of the position and velocity errors are an order of magnitude lower than those of the survey-grade Blue Logger recording carrier phase information Ashtech (BLASH) GPS configuration (MacMahan et al. 2009), which has the ability to resolve flows in the order of $0.05\,\mathrm{m\,s^{-1}}$. The low magnitude of these errors demonstrates the ability of the present drifters to obtain accurate

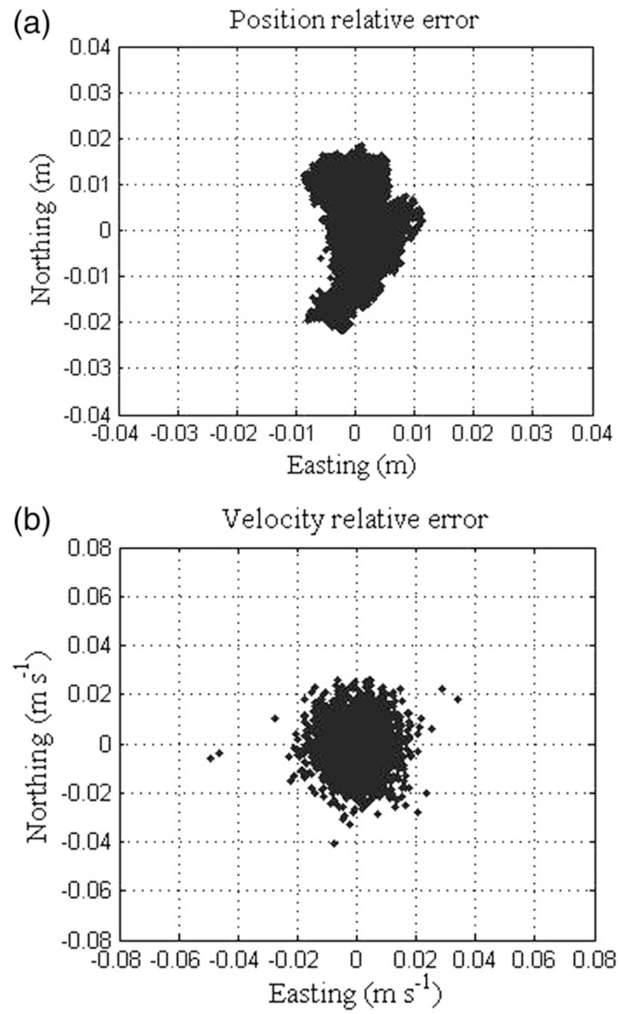

FIG. 3. Relative error obtained from stationary measurements for test 1: (a) positions in north and east directions and (b) velocities in east (V_e) and north (V_n) directions. See Table 2 for results for tests 2 and 3.

position and velocity measurements [$O(0.09\,\mathrm{m\,s^{-1}})$], that is, an order of magnitude greater than the maximum velocity error) for describing the dispersion process in estuarine environments where processes of interest occur at small scales [$O(100\,\mathrm{s})$ and O(few meters)].

6. GPS error removal and drifter field performance

The removal of GPS errors existing at high frequency from actual position data can be done by means of low-pass filtering of the RTK positioning solution. This requires defining the cutoff frequency, where the signal-to-noise ratio (SNR) is less than an acceptable value. For resolving environmental flow scales, SNR must be greater than 10; that is, the true signal should be at least an order of magnitude larger than the device noise

TABLE 2. Statistics of stationary tests from different locations; test 1 results are presented in Fig. 3.

Test	Distance from the reference station	Maximum position error (cm)		Std dev of position error (cm)		Maximum velocity error (cm s^{-1})		Mean velocity error (cm s^{-1})		Std dev of velocity error (cm)	
		North	East	North	East	North V_n max	East V_e max	North V_n	East V_e	North V_n std	East V_e std
1	~40 m	2.50	1.80	1.00	0.83	5.58	2.90	0.0034	−0.0021	0.73	0.56
2	~50 m	2.20	1.10	0.86	0.32	4.00	4.95	−0.0013	0.00042	0.54	0.43
3	~16 km	2.50	1.55	0.53	0.85	4.96	6.00	0.00033	0.00058	0.69	0.94

(Johnson et al. 2003; Johnson and Pattiaratchi 2004; MacMahan et al. 2009). The data from the drifter test 3 at Eprapah Creek (Table 1) were used for field performance spectra analysis. The stationary observations were uncorrelated with the field-deployed observations; thus, we define the spectrum of the true observations as

$$S_{\mathrm{xx}} = S_{\mathrm{XX}} - S_{\mathrm{rr}}, \tag{3}$$

where $S_{\mathrm{rr}} = S_{\mathrm{XX}}|_{x=0}$ is the spectrum of stationary observation and S_{xx} is the spectrum of field observation. SNRs were then obtained from Eq. (4):

$$\mathrm{SNR}(f) = \frac{S_{\mathrm{XX}}(f) - S_{\mathrm{rr}}(f)}{S_{\mathrm{rr}}(f)}. \tag{4}$$

The spectra of positions and velocities were obtained by fast Fourier transform (FFT), described in Johnson and Pattiaratchi (2004). The length of field observation equivalent to the stationary observation was used in computing the SNR in order to maintain the same frequency resolution. The position and velocity spectra (Fig. 4) were computed as the average of eight overlapping sections of 4096 points Hanning windowed at the 95% confidence level. The position spectra of the stationary measurement are similar in shape and trend with those obtained by Johnson et al. (2003), Johnson and Pattiaratchi (2004), and MacMahan et al. (2009), with magnitudes of $O(0.01\,\mathrm{m}^2\,\mathrm{s})$. The lower magnitude is indicative of the lower relative error when compared to previous drifters applied in larger water bodies. The slope of the relative error position power spectral density (PSD) between 0.001 and 0.01 Hz is best fitted with a power of 1 compared with 1.3 observed by Johnson et al. (2003).

The position of the SNR (Fig. 4e) shows that the noise level is insignificant at low frequencies—especially below 1 Hz, where the true signal is of an order of magnitude higher. The SNR went below 10 at frequencies beyond 1.5 Hz in both streamwise and cross-shore directions. This suggests a cutoff frequency of $f_c = 1.5$ Hz, as compared to a survey-grade drifter applicable to rip currents with a cutoff frequency of $O(0.1\,\mathrm{Hz})$ (BLASH configuration; MacMahan et al. 2009). The SNR of several other portions of the field data was also tested, with all indicating acceptable observations of frequency up to the range of 1–2 Hz. This high cutoff frequency enables studying shallow water dispersion processes of interest occurring at a frequency of $O(1\,\mathrm{Hz})$. Further analysis of the data was done by application of low-pass filter on the quality-controlled data using the computed cutoff frequencies. This approach removes the high-frequency content of the data where the magnitude of error is high.

The velocity SNR reveals that the drifter cross-shore velocity data were corrupted with noise from a frequency of 0.1 Hz upward, while there was significant signal level in streamwise velocities up to 1.5 Hz due to the low cross-shore velocity of the tidal channel.

The velocities of the drifters were compared with the fixed ADVs and the ADCP sampled at transects 10.1 m apart (Fig. 5). There is difficulty in validating the drifter measurements with Eulerian data (ADVs and ADCP) on the field because these devices experience similar velocity only for short times. In addition, in shallow estuaries, the combined effects of tide, wind, and bathymetry result in high spatial variability of velocities. In spite of these factors, the drifter shows a similar trend in time with that of the ADVs when the drifter was within a 50-m streamwise radius of the ADVs. The large values of drifter streamwise velocity are probably related to both the wind shear on the subsurface layer of the estuary and unavoidable wind drag on the unsubmerged portion of the drifter. Figure 5b shows the postprocessed ADCP ensembled streamwise velocity at centered time, $t = 119\,100$ s, and the average of the time series (ADV and GPS drifter) is shown in Fig. 5a. The vertical profile of the channel streamwise velocity shows that the velocity increased with relative height from the bed, similar to steady wide open channel flow with a maximum velocity close to the surface as indicated by the drifter velocity and the ADCP bins next to the free surface. This additionally validates that the drifter motion is representative of the near-surface horizontal current motion. The correlation of drifter velocity in the cross-shore direction was poor, as a result of secondary flows in the semicircular meander (sites 2B and 2BB in Fig. 2), which the drifter could not properly resolve.

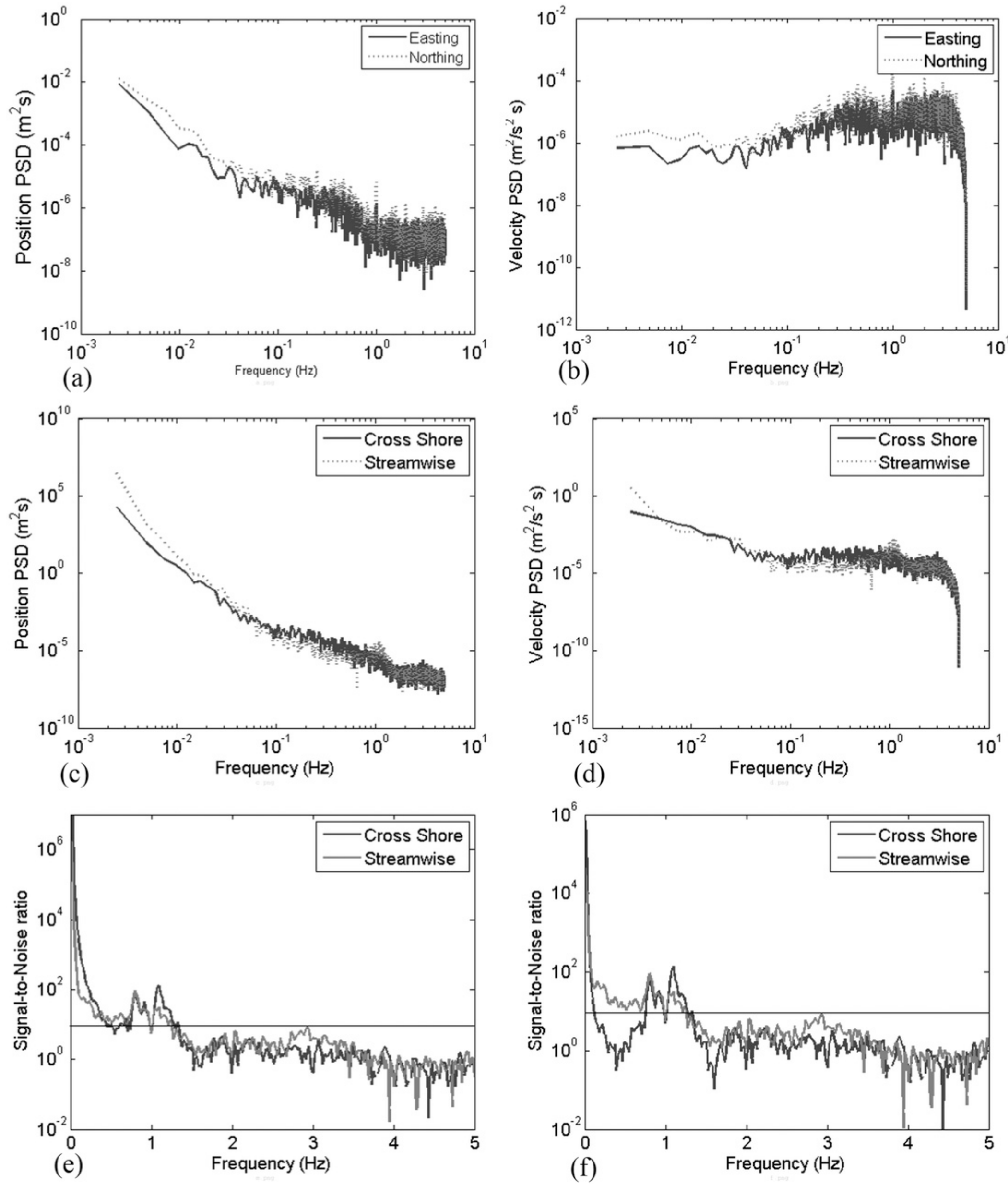

FIG. 4. Spectral analyses of a 34-min signal. (a) Relative position error from stationary record, converted to local east and north coordinates. (b) Velocity computed from stationary records. (c) Field observation in local streamwise and cross-shore coordinates. (d) Velocity for field deployment. All power spectral densities are averaged estimates of eight 50% overlapping sections of 4096 points with each section windowed with a Hanning window. (e) SNR for the displacement measurement and (f) SNR for the velocity measurement using the drifter.

7. Diffusion estimate

Statistical analysis of Lagrangian data is mostly concerned with either single particles or the relative motion of groups of particles (Berti et al. 2011). Single particle analysis of tracked drifters has been used to identify the underlining dynamics in the atmospheres and oceans (LaCasce 2008). The basic application of single particle analysis to an estuarine environment is the estimate of the absolute diffusivity.

The horizontal position coordinates of the quality-control data (Table 1; test 1) were low-pass filtered with a cutoff frequency of $f_c = 1.5$ Hz. The decorrelation time scale for the individual drifters was estimated from the autocorrelation function of residual velocities obtained upon removal of the averaged velocity and was found to

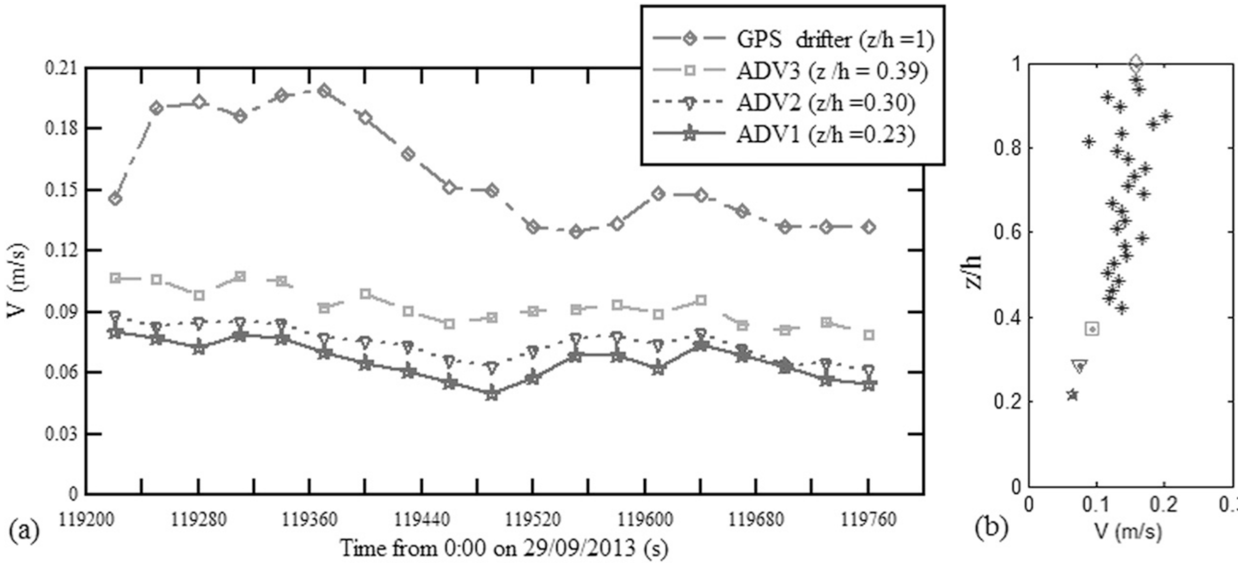

FIG. 5. (a) Eprapah Creek streamwise velocity profiles (Table 1; test 2) averaged over 30 s measured by the GPS drifter. (b) Vertical profile of average streamwise velocity as a function of height z from the bed normalized by water depth h, where the asterisks indicate values measured by the upward-looking ADCP placed on the stream bed, 10.1 m downstream of the ADV transect. The GPS drifter was within 50 m streamwise of the ADV transect.

be 50 and 15 s in the streamwise and cross-shore directions, respectively. The diffusivity estimates proceeded with the basic assumptions of homogeneity and stationarity of the residual flow field. Therefore, the position time series were separated into short independent realizations with time intervals greater than the decorrelation time to obtain the displacement time series. Figure 6 shows 20 realizations of the displacement time series, each of 10 min long. The normalized density of the displacement time series gives the probability distribution function (PDF). The variances (absolute dispersions) were estimated from the PDF, thence the absolute diffusivity, which is the rate of absolute dispersion with time. Herein, the absolute dispersion coefficient is obtained as the slope of absolute dispersion with respect to time by linear regression for times $t > 100$ s, times greater than the decorrelation time scale (Taylor 1921; Berti et al. 2011). The dispersion coefficient varied with the length of short realizations. The maximum absolute streamwise dispersion coefficient $K_{ss} = 0.57\,\mathrm{m^2\,s^{-1}}$ was obtained with 16-min realization length, while that of the cross-shore direction $K_{nn} = 0.053\,\mathrm{m^2\,s^{-1}}$ was obtained with 5.6-min realization length.

Many prior estimates of estuarine–coastal water diffusivity used observation from tracer dyes to obtain dispersion coefficients. The minimum lateral dispersion coefficient for 19 sites in the United Kingdom ranged from 0.003 to $0.42\,\mathrm{m^2\,s^{-1}}$ (Riddle and Lewis 2000). Unlike the present observation, where the ensemble average of the group of realizations is used in the estimate, the values reported by Riddle and Lewis (2000) were based on individual realizations. Despite the differences in approach, the lateral dispersion coefficient, $K_{nn} = 0.028\,\mathrm{m^2\,s^{-1}}$, in the present work is within range. The values $K_{ss} = 0.57\,\mathrm{m^2\,s^{-1}}$ and $K_{nn} = 0.053\,\mathrm{m^2\,s^{-1}}$ are also in range with estimates using the GPS drifter in North Fork Skagit River—a similar meandering river in the United States—where $K_{ss} = 0.39\,\mathrm{m^2\,s^{-1}}$ and $K_{nn} = 0.09\,\mathrm{m^2\,s^{-1}}$ were obtained. Table 3 shows the estimates of dispersion coefficient in similar shallow water bodies.

Using the displacement time series shown in Fig. 6, higher-order moments of the displacement PDF were calculated. The skewness has nonzero values ranging from −0.8 to 0.4 in the cross-shore direction and between 0.4 and 0.8 in the streamwise direction. This is a result of inhomogeneity of the dataset. The values of kurtosis in the cross-shore direction are not significantly different from 3, the expected value for normal distribution. In addition, the cross-shore diffusion coefficient decreased with an increase in the length of realizations beyond 5.6 min. These results suggest that the cross-shore spreading is subdiffusive at times greater than 5.6 min. On the other hand, the kurtosis values are mostly around 2.5 in the streamwise direction and the diffusion coefficient increased with longer segments. These suggest that the streamwise displacement contains strong advection and is superdiffusive.

8. Limitations and benefits of present GPS drifter

The use of a GPS-tracked drifter in studying the dynamics of shallow coastal water has many advantages

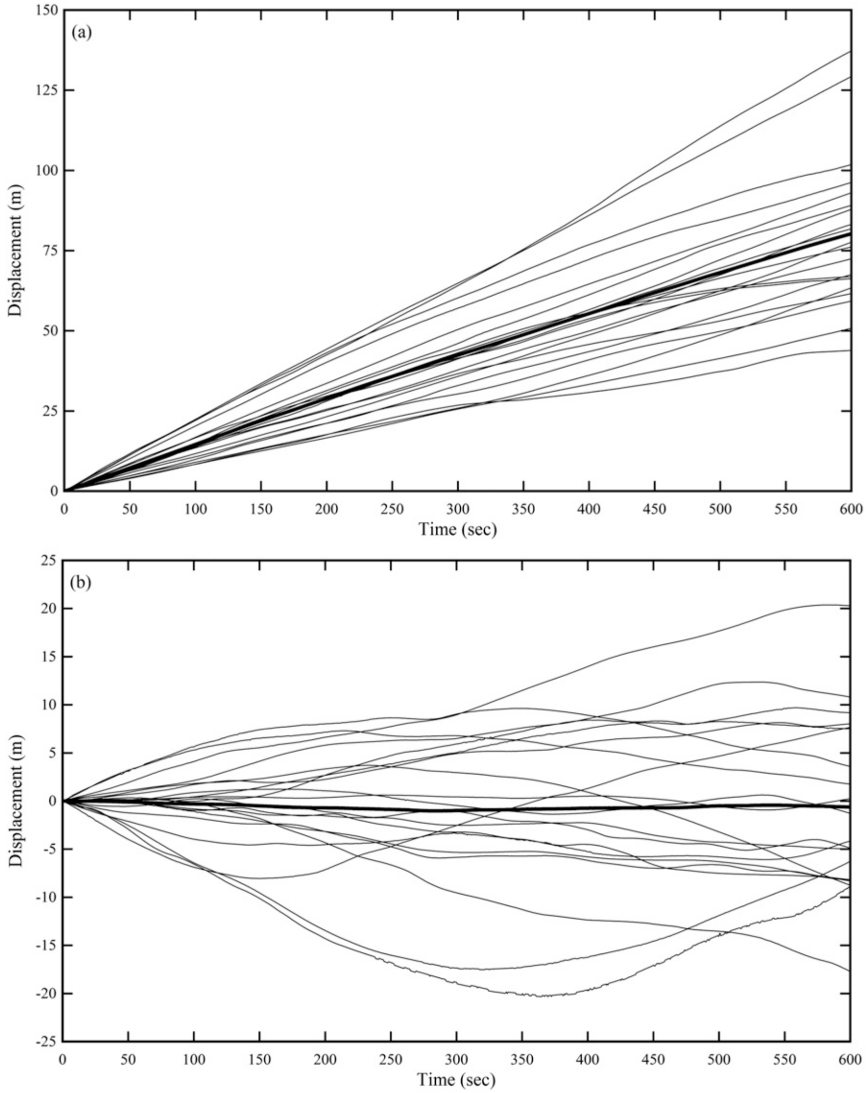

FIG. 6. Displacement time series for segmented drifter trajectories with average displacement in bold: (a) streamwise component and (b) cross-shore component.

over existing dye tracer technology and acoustic Eulerian devices, including flexibility of usage, lower cost, and higher spatial coverage. Despite these advantages, there are methodical and practical limitations with this application. These limitations include but are not limited to the inevitable wind-induced pseudo-Lagrangian behavior, the inability of the drifter to resolve small-scale motion, and the irresponsiveness of the drifter to the true vertical motion. Although the present drifter is designed such that only 30-mm height is exposed to direct wind drag, the wind effect could inconsistently influence the path of the drifter. This false movement, however, could not be totally eliminated and thus requires consideration when interpreting results from drifter studies, particularly in low current speed applications. The present drifter configuration has a drag area ratio of 8.5–13 and a velocity difference attributed to wind of less than 1% of wind speed using a simple empirical model (Niiler and Paduan 1995). The drifter configuration is designed for shallow water bodies with relatively small wave motion. Application of the drifter to deeper water bodies requires a slight modification that includes the addition of a window shade or parachute drogues to increase the drag area ratio and to reduce the effects of wave rectification.

In environmental flows, the scale of motion ranges from the energy containing large eddies (mean flow) to the smallest eddies (turbulent fluctuations). A drifter functions as a filter that only captures motion on a scale greater than its radius. Thus, the drifter size limits the

TABLE 3. Diffusivity estimates for shallow riverine and estuarine environment based on dye tracer technology and evolving GPS-tracked drifter technology.

Location	Year	Method	Tidal current (m s^{-1})	Depth (m)	Cross-shore K_{nn} (m^2 s^{-1})	Streamwise K_{ss} (m^2 s^{-1})	Source
Irvin Bay, United Kingdom*	1972	Dye tracer	0.06	6	0.05	—	(Riddle and Lewis 2000)
Plym Estuary, United Kingdom*	1973	Dye tracer	0.15	4	0.01	—	(Riddle and Lewis 2000)
Tee Estuary, United Kingdom*	1978	Dye tracer	0.15	3	0.05	—	(Riddle and Lewis 2000)
Poole Estuary, United Kingdom* (flood tide)	1979	Dye tracer	0.75	1.8	0.014	—	(Riddle and Lewis 2000)
Yantze–China	1999	Dye tracer	0.5	5	0.88	—	(Riddle and Lewis 2000)
North Fork Skagit, United States	2008	GPS drifter	0.55	—	0.09	0.39	(Swick and MacMahan 2009)
Upper estuary, Eprapah Creek, Australia (flood tide)	2013	GPS drifter	0.14	3	0.053	0.57	Present study

* Values are minimum estimates for the area.

range of eddies captured. Similarly, the high noise level at the high frequency obtained from evaluation imposes limits (cutoff frequencies) on the frequency content that the drifter could reliably acquire. A relevant dataset is the eddy viscosity data reported by Trevethan et al. (2006) with eddy viscosities between 0.000 01 and 0.001 m^2 s^{-1}. The eddy viscosity is two orders of magnitude lower than the dispersion coefficients obtained with the GNSS-tracked drifters, suggesting large a Péclet number in drifter motion, that is, a large dispersion-to-diffusion ratio. Likewise, limitations in vertical motion as a result of constant density of the drifter are a clear disadvantage of drifter dispersion when compared with tracer dye dispersion, which mixes both vertically and horizontally. Thus,

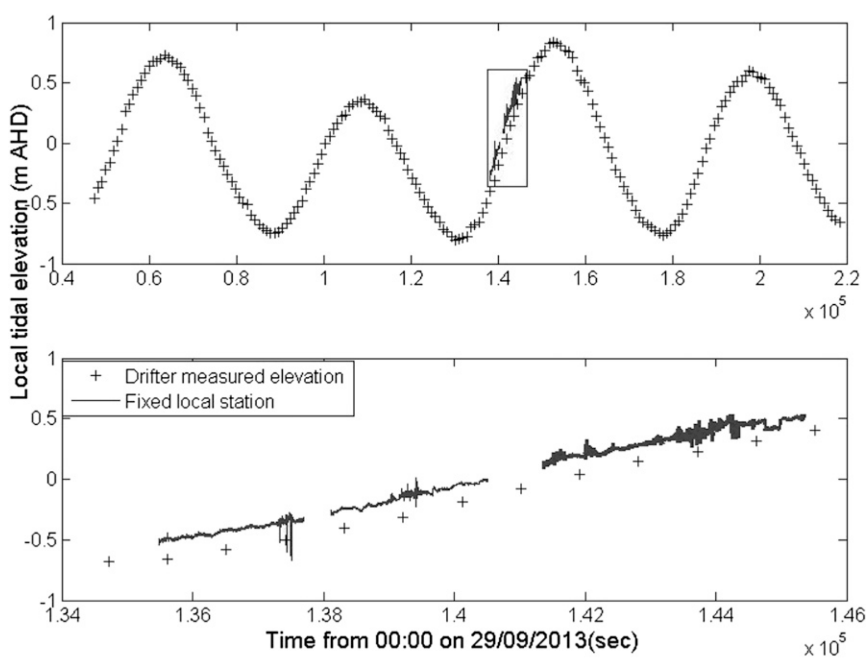

FIG. 7. (top) Eprapah Creek tidal elevation between 29 Sep and 1 Oct 2013 obtained from survey staff close to the ADV at site 2BB, corrected to mAHD based on height of the Victoria Point station above the lowest astronomic tides. (bottom) Rectangular-boxed area in (a) showing drifter-measured elevation (+ signs), despiked, and low-passed filtered at 0.5 Hz. Each of the three segments denotes a separate run. The solid line segments represents the elevation from a fixed local station. All times synchronized in seconds and taken from 0000 Australian standard time 29 Sep 2013.

surface-only observation gives a biased approximation of the estuarine mixing as a two-dimensional phenomenon.

Though vertical displacement of drifters does not amount to dispersion, drifters move with the rise and fall of the current. The high resolution of the present drifter makes it sensitive to displacement as low as 1 cm. The upward displacements were obtained from the transformation from GPS height to mAHD using AUSGeo09 as detailed in Brown (2010) after which a low-pass filter with a cutoff frequency of 0.5 Hz was applied to eliminate noise at high frequency. Figure 7 shows the plot of the tidal elevation from the GPS validated with the local tidal elevation in AHD against the synchronized time. The drifter data compares well with the local tidal elevation. In addition, a low-frequency wave causing the rise and fall in the tidal height is observed, which could be analyzed to establish its contribution to the overall mixing in the water body. This makes the present drifter modifiable for flood height monitoring, where drifters could be free floating or moored while providing real-time, near-continuous height and flow dynamics information.

9. Conclusions

The advancements in GNSS–RTK coupled technology have paved the way for centimeter-resolution tracking, thus allowing the study of finescale flow dynamics at higher temporal resolution compared to existing drifters. Field studies were conducted using the newly developed drifters in a shallow estuary, Eprapah Creek, at Victoria Point, Queensland, Australia. Data obtained from both the stationary and field studies provided an estimate of the SNR where the drifter showed efficient performance up to a frequency of 1.5 Hz for displacement measurement. Single particle analysis was used to obtain the absolute dispersion from several realizations, hence diffusivities ($K_{ss} = 0.57\,\mathrm{m^2\,s^{-1}}$ and $K_{nn} = 0.053\,\mathrm{m^2\,s^{-1}}$), are obtained that agree well with the estimate for similar water bodies. Further field deployments of the developed drifters are being carried out at Eprapah Creek to estimate the spatial and temporal variability of dispersion coefficients along the tidal channel. The vertical position coordinates of the field deployment reveal that high-resolution GPS-tracked drifters are applicable to flood height monitoring. An extensive study using both dye tracer and drifters under the same condition is required to quantify the compromise of surface-only dispersion estimates in shallow water estuaries.

Acknowledgments. The authors wish to thank all the people who participated in the field study; those who assisted with the preparation and data analysis; and the Queensland Department of Natural Resources and Mines, Australia, for providing access to the SunPOZ network for reference station data used for RTK postprocessing.

REFERENCES

Berti, S., F. A. D. Santos, G. Lacorata, and A. Vulpiani, 2011: Lagrangian drifter dispersion in the southwestern Atlantic Ocean. *J. Phys. Oceanogr.,* **41,** 1659–1672, doi:10.1175/2011JPO4541.1.

Brown, N., 2010: AusGeoid09: Converting GPS heights to AHD heights. *Ausgeo News,* No. 97, Geoscience Australia, Symonston, ACT, Australia, 1–3.

Chanson, H., 2004: *Environmental Hydraulics of Open Channel Flows.* Elsevier-Butterworth-Heinemann, 430 pp.

——, R. Brown, and M. Trevethan, 2012: Turbulence measurements in a small subtropical estuary under king tide conditions. *Environ. Fluid Mech.,* **12,** 265–289, doi:10.1007/s10652-011-9234-z.

——, B. Gibbes, and R. J. Brown, 2014: Turbulent mixing and sediment processes in peri-urban estuaries in South-East Queensland (Australia). *Estuaries of Australia in 2050 and Beyond,* Estuaries of the World, E. Wolanski, Ed., Springer, 167–183.

D'Roza, T., and G. Bilchev, 2003: An overview of location-based services. *BT Technol. J.,* **21,** 20–27, doi:10.1023/A:1022491825047.

Fischer, H. B., E. J. List, R. C. Y. Koh, J. Imberger, and N. H. Brooks, 1979: *Mixing in Inland and Coastal Waters.* Academic Press, 302 pp.

Johnson, D., and C. Pattiaratchi, 2004: Application, modelling and validation of surfzone drifters. *Coastal Eng.,* **51,** 455–471, doi:10.1016/j.coastaleng.2004.05.005.

——, R. Stocker, R. Head, J. Imberger, and C. Pattiaratchi, 2003: A compact, low-cost GPS drifter for use in the oceanic nearshore zone, lakes, and estuaries. *J. Atmos. Oceanic Technol.,* **20,** 1880–1884, doi:10.1175/1520-0426(2003)020<1880:ACLGDF>2.0.CO;2.

Kopasakis, K. I., A. N. Georgoulas, P. B. Angelidis, and N. E. Kotsovinos, 2012: Numerical modeling of the long-term transport, dispersion, and accumulation of Black Sea pollutants into the North Aegean coastal waters. *Estuaries Coasts,* **35,** 1530–1550, doi:10.1007/s12237-012-9540-9.

LaCasce, J., 2008: Lagrangian statistics from oceanic and atmospheric observations. *Transport and Mixing in Geophysical Flows: Creators of Modern Physics,* J. B. Weiss and A. Provenzale, Eds., Lecture Notes in Physics, Vol. 44, Springer, 165–218.

Landry, M. R., M. D. Ohman, R. Goericke, M. R. Stukel, and K. Tsyrklevich, 2009: Lagrangian studies of phytoplankton growth and grazing relationships in a coastal upwelling ecosystem off Southern California. *Prog. Oceanogr.,* **83,** 208–216, doi:10.1016/j.pocean.2009.07.026.

Legleiter, C. J., and P. C. Kyriakidis, 2006: Forward and inverse transformations between Cartesian and channel-fitted coordinate systems for meandering rivers. *Math. Geol.,* **38,** 927–958, doi:10.1007/s11004-006-9056-6.

List, E. J., G. Gartrel, and C. D. Winant, 1990: Diffusion and dispersion in coastal waters. *J. Hydraul. Eng.,* **116,** 1158–1179, doi:10.1061/(ASCE)0733-9429(1990)116:10(1158).

Lumpkin, R., and M. Pazos, 2007: Measuring surface currents with Surface Velocity Program drifters: The instrument, its data, and some recent results. *Lagrangian Analysis and Prediction of Coastal and Ocean Dynamics,* A. Griffa et al., Eds., Cambridge University Press, 39–67.

MacMahan, J., J. Brown, and E. Thornton, 2009: Low-cost handheld global positioning system for measuring surf-zone currents. *J. Coastal Res.,* **253,** 744–754, doi:10.2112/08-1000.1.

Niiler, P. P., and J. D. Paduan, 1995: Wind-driven motions in the northeast Pacific as measured by Lagrangian drifters. *J. Phys. Oceanogr.,* **25,** 2819–2830, doi:10.1175/1520-0485(1995)025<2819:WDMITN>2.0.CO;2.

Ohlmann, J. C., J. H. LaCasce, L. Washburn, A. J. Mariano, and B. Emery, 2012: Relative dispersion observations and trajectory modeling in the Santa Barbara Channel. *J. Geophys. Res.,* **117,** C05040, doi:10.1029/2011JC007810.

Pal, B. K., R. Murthy, and R. E. Thomson, 1998: Lagrangian measurements in Lake Ontario. *J. Great Lakes Res.,* **24,** 681–697, doi:10.1016/S0380-1330(98)70854-8.

Poje, A. C., and Coauthors, 2014: Submesoscale dispersion in the vicinity of the *Deepwater Horizon* spill. *Proc. Natl. Acad. Sci. USA,* **111,** 12 693–12 698, doi:10.1073/pnas.1402452111.

Qiu, Z. F., A. M. Doglioli, Z. Y. Hu, P. Marsaleix, and F. Carlotti, 2010: The influence of hydrodynamic processes on zooplankton transport and distributions in the North Western Mediterranean: Estimates from a Lagrangian model. *Ecol. Modell.,* **221,** 2816–2827, doi:10.1016/j.ecolmodel.2010.07.025.

Riddle, A. M., and R. E. Lewis, 2000: Dispersion experiments in U.K. coastal waters. *Estuarine Coastal Shelf Sci.,* **51,** 243–254, doi:10.1006/ecss.2000.0661.

Schmidt, W., B. Woodward, K. Millikan, R. Guza, B. Raubenheimer, and S. Elgar, 2003: A GPS-tracked surf zone drifter. *J. Atmos. Oceanic Technol.,* **20,** 1069–1075, doi:10.1175/1460.1.

Schroeder, K., and Coauthors, 2012: Targeted Lagrangian sampling of submesoscale dispersion at a coastal frontal zone. *Geophys. Res. Lett.,* **39,** L11608, doi:10.1029/2012GL051879.

Situ, R., and R. J. Brown, 2013: Mixing and dispersion of pollutants emitted from an outboard motor. *Mar. Pollut. Bull.,* **69,** 19–27, doi:10.1016/j.marpolbul.2012.12.015.

Spydell, M., and F. Feddersen, 2009: Lagrangian drifter dispersion in the surf zone: Directionally spread, normally incident waves. *J. Phys. Oceanogr.,* **39,** 809–830, doi:10.1175/2008JPO3892.1.

Stocker, R., and J. Imberger, 2003: Horizontal transport and dispersion in the surface layer of a medium-sized lake. *Limnol. Oceanogr.,* **48,** 971–982, doi:10.4319/lo.2003.48.3.0971.

Sundermeyer, M. A., and J. R. Ledwell, 2001: Lateral dispersion over the continental shelf: Analysis of dye release experiments. *J. Geophys. Res.,* **106,** 9603–9621, doi:10.1029/2000JC900138.

Swick, W., and J. MacMahan, 2009: The use of position-tracking drifters in riverine environments. *OCEANS 2009, MTS/IEEE Biloxi—Marine Technology for Our Future: Global and Local Challenges,* IEEE, 1–10.

Takasu, T., and A. Yasuda, 2009: Development of the low-cost RTK-GPS receiver with an open source program package RTKLIB. *Int. Symp. on GPS/GNSS,* Jeju, South Korea, Korean GNSS Technology Council, 6 pp. [Available online at http://gpspp.sakura.ne.jp/paper2005/isgps_2009_rtklib_revA.pdf.]

Taylor, G. I., 1921: Diffusion by continuous movements. *Proc. London Math. Soc.,* **20,** 196–212, doi:10.1112/plms/s2-20.1.196.

Trevethan, M., H. Chanson, and R. Brown, 2006: Series of detailed turbulence measurements in a small subtropical estuarine system. University of Queensland Tech. Rep. CH58/06, 156 pp.

——, ——, and ——, 2008: Turbulence characteristics of a small subtropical estuary during and after some moderate rainfall. *Estuarine Coastal Shelf Sci.,* **79,** 661–670, doi:10.1016/j.ecss.2008.06.006.